Geofísica Internacional (2012) 51-1: 63-72

Original paper

A case of study for Pseudorange multipath estimation and analysis: TAMDEF GPS network

Guadalupe Esteban Vázquez B.* and Dorota A. Grejner-Brzeziska

Received: January 31, 2011; accepted: June 7, 2011; published on line: December 16, 2011

Resumen

Un estudio de investigación se llevó a cabo para evaluar la cantidad del efecto de multiruta en pseudo-distancias a partir de observaciones GPS (Sistemas de Posicionamiento Global) en la red TAMDEF (Montañas Trans Antárticas), situadas en la región de Victoria en la Antártica y que consta de 33 estaciones GPS. Es bien sabido que, a pesar de la selección cuidadosa de los lugares para el establecimiento de estaciones GPS, éstas son en cierta medida afectadas por el efecto de multiruta. El efecto de multiruta para mediciones GPS de pseudo-distancias puede ser entonces una contribución potencial que podría tener un impacto en el posicionamiento de las estaciones TAMDEF. De tal manera que, las variaciones de los errores medios cuadráticos (MP1-RMS y MP2-RMS) fueron estimadas y analizadas a fin de identificar las estaciones con mayor y menor índice de afectación, considerando datos GPS desde el año 1996 hasta el año 2006. La estación McMurdo (MCM4) del IGS fue incluida como parte de la red TAMDEF, tomando en cuenta que ésta es considerada el punto principal de acceso al ITRF (Marco de Referencia Terrestre Internacional) para esta parte de la Antártica.

Palabras clave: pseudo-distancia, multiruta, GPS, TAMDEF, Antártica.

Abstract

A research study was conducted to evaluate the amount of pseudorange multipath from GPS (Global Positioning System) observables at TAMDEF (Trans Antarctic Mountain Deformation) network, located in Victoria Land, Antarctica consisting of 33 GPS stations. It is well known that, despite carefully selected locations, the GPS stations are to some extent, affected by the presence of multipath. Pseudorange multipath effect for GPS measurements could be a potential contributor that might have an impact on the TAMDEF stations positioning. Thus, the root mean squared error variations (MP1-RMS and MP2-RMS) were estimated and analyzed in order to identify the most and least affected sites, considering GPS data span from year 1996 to year 2006. McMurdo (MCM4) IGS (The International GNSS Service for Geodynamics, formerly the International GPS Service) site, was adopted as part of the TAMDEF network, since MCM4 is the primary ITRF (International Terrestrial Reference Frame) access point for this part of Antarctica.

Key words: Pseudorange, multipath, GPS, TAMDEF, Antarctica.

G. Esteban Vázquez B.
Escuela de Ciencias de la Tierra de la Universidad Autónoma de Sinaloa
Culiacán, México
*Corresponding author: estebanv_99@yahoo.com

Dorota A. Grejner-Brzeziska
Satellite Positioning and Inertial Navigation
SPIN Laboratory
The Ohio State University

Introduction

The TAMDEF Network is a GPS array deployed on bedrock, consisting of 25-campaign sites, 6-quasi-continuous sites and 2-continuous sites (see Figure 1), located in the Trans Antarctic Mountains of the southern Victoria Land and on the islands in the adjacent Ross Sea. TAMDEF is the OSU (Ohio State University) and USGS (United States Geological Survey) joint project sponsored by the NSF (National Science Foundation), initiated in 1996 with the primary objective to measure vertical and horizontal crustal deformation (http://www.geology.ohio-state.edu/TerryWilson/research_gps.htm). At the present time, some of the TAMDEF sites are part of the related POLar Earth observing NETwork (POLENET) which is expected to be an ambitious international project to understand geophysical aspects at very remote high-latitude such as the Antarctic continent (http://www.polenet.org/).

Despite their careful selection, the TAMDEF GPS sites are, to some extent, affected by the presence of local multipath effects. This effect may vary slowly on a seasonal basis, or abruptly due to such natural events as snowfall. Studies of multipath effects and suitable processing

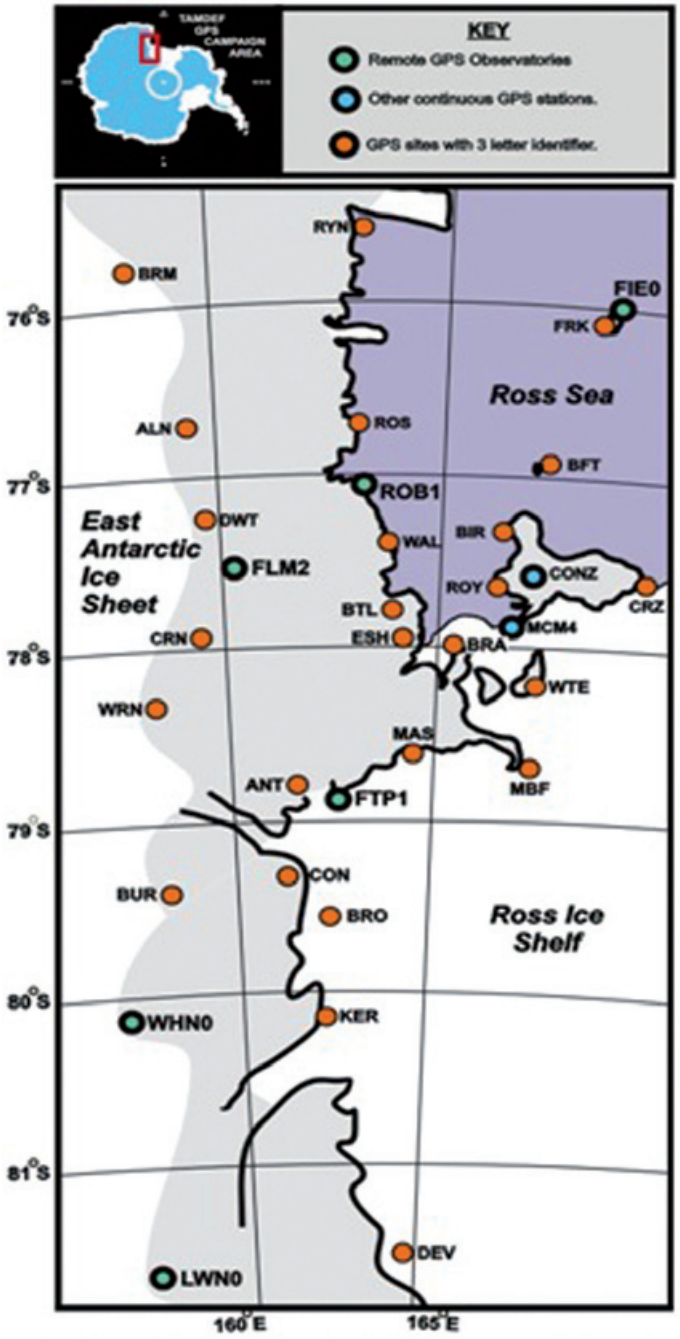

Figure 1. TAMDEF GPS network, located in the Trans Antarctic Mountains of the southern Victoria Land and on the islands in the adjacent Ross Sea.

techniques are given, for example, by Han and Rizos (1997), Rizos (1999), Meertens (2000), Ge *et al*. (2000), Dodson *et al*. (2001), Roberts *et al*. (2002), Ge *et al*. (2002) and Satirapod *et al*. (2003). It is important to indicate here that all of the methods cited above have their advantages and limitations; however, it is been shown in the above-cited literature that the multipath error in the pseudoranges is significantly larger (up to several meters) than for carrier phases (usually, millimeter to centimeter level).

Since the multipath effect depends on the satellite geometry and the surrounding environment of the GPS antenna (as well as the antenna type), it is practically the same after one sidereal day under similar atmospheric conditions. In other words, with the current GPS orbit design, the entire satellite configuration normally advances about 4 minutes between two consecutive days. Thus, the positioning solution of data derived from the repetition of the GPS satellite constellation between two sidereal days ought to be affected by "systematic" multipath. This effect can be used to extract the multipath signature from the positioning time-series (Ge *et al*., 2000, Roberts *et al*., 2002). Hilla and Cline (2002) pointed out that the significance of analyzing pseudorange multipath is that the accuracy of any GPS application relies to a large extent on pseudorange measurements (e.g., differential pseudorange, kinematic and rapid static surveying, and ionospheric monitoring). Therefore, in order to identify the effective level of multipath, the daily MP1-RMS and MP2-RMS variations were estimated and analyzed at each TAMDEF site.

TAMDEF GPS instrumentation

TAMDEF hardware consists of a wide variety of dual-frequency, 12-20 channel, geodetic-grade GPS receivers, kept in insulated boxes and powered from 60W solar panels and 80 amp-hours gel-cell batteries. The GPS receivers used in the TAMDEF network are: Trimble 5700/R7, Ashtech Z-Surveyors, DL4-NovAtel, Leica RS500, Javad Legacy and Javad Euro-80. The GPS receivers, supplied through cooperation with USGS, OSU and UNAVCO (University NAVstar COnsortium), are usually set to record data every 30 seconds in the field without any replacement of their memory cards. To allow for consistency, the TAMDEF team places the same antenna type at each site each year. TAMDEF almost exclusively uses Ashtech/Thales Dorne-Margolin (D&M) choke-ring antenna designed to reduce L1 multipath. This type of antenna is used because it accepts a wide range of input voltages, and it has also been tested to be consistent for possible phase center variations when using the antenna calibration parameters provided by NGS (National Geodetic Survey) (http://www.grdl.noaa.gov/ANTCAL/).

GPS data availability and data processing

When TAMDEF network was first established, only GPS data for a short of time period (1 or 2 weeks) was available. However, this has improved over the past few years and data from some permanent quasi-continuous (with 1 to 3 months of data) and also continuous trackers (with almost the entire year of data) are now accessible for further processing. Figure 2 illustrates TAMDEF station data availability for those sites (FLM2: Mount Fleming 2; FTP1: Fishtail Point 1; LWN0: Lonewolf Nunatak; MCM4: McMurdo; ROB1: Cape Roberts; WHN0: Westhaven Nunatak) with longer GPS data span from 1996 to 2005, hereinafter called "tested" sites.

The TAMDEF GPS data were converted and archived to the RINEX (Receiver INdependent EXchange) format (ftp://igscb.jpl.nasa.gov/igscb/data/format/rinex210.txt). The TEQC software (Test of Quality Check) provided by UNAVCO, which is also available for public use at (http://www.unavco.org/facility/software/teqc/teqc.html), was used to verify the quality and integrity of the RINEX files and to estimate the daily root mean squared variations for each analyzed TAMDEF site. The main specifications for the GPS data processing included the use of a 30-sec sampling rate and 10° cut-off angle.

Pseudorange multipath estimation

It is important to point out, that in the one-way observation equations used for the multipath estimation, the inter-channel bias and the non-integer initial phase terms for the satellite and the receiver were neglected. This research follows the pseudorange multipath approach proposed by Estey and Meertens (1999); Hilla and Cline (2002); http://www.unavco.org QC V3 Users Guide, UNAVCO 1994. The pseudorange and carrier phase measurements on L1 and L2 for a satellite (κ) and a receiver (i) are given by:

$$P_{L1} = R + c(\quad t^k - \quad t_i) + I_{L1} + T + MP_{P1} \tag{1}$$

$$P_{L2} = R + c(\quad t^k - \quad t_i) + I_{L2} + T + MP_{P2} \tag{2}$$

$$\Phi_{L1} = R + c(\quad t^k - \quad t_i) + \lambda_{L1} N_{L1} - I_{L1} + T + MP_{\Phi_{L1}} \tag{3}$$

$$\Phi_{L2} = R + c(\quad t^k - \quad t_i) + \lambda_{L2} N_{L2} - I_{L2} + T + MP_{\Phi_{L2}} \tag{4}$$

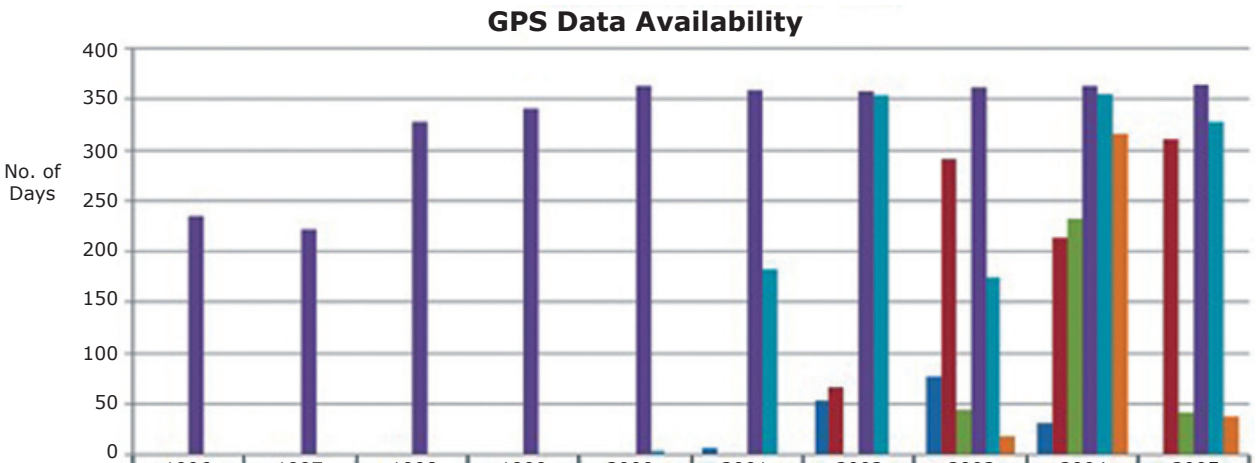

	1996	1997	1998	1999	2000	2001	2002	2003	2004	2005
FLM2	0	0	0	0	0	6	53	76	31	0
FTP1	0	0	0	0	0	0	66	291	214	311
LWN0	0	0	0	0	0	0	0	44	232	41
MCM4	235	222	328	341	363	359	357	361	363	364
ROB1	0	0	0	0	3	183	353	174	355	328
WHND	0	0	0	0	0	0	0	18	316	38

Figure 2. GPS data availability for "tested" (with longer GPS data span) TAMDEF sites.

where: P_{L1} and P_{L2} are the pseudorange observations (in meters), ϕ_{L1} and ϕ_{L2} are the corresponding carrier phase observations on L1 and L2, respectively, R is the geometric distance between the satellite and the receiver (in m), c is the constant speed of light (in m/s), Δt_i is the satellite clock correction (in s), Δt^k is the receiver clock correction (in s), I_{L1} and I_{L2} are the ionospheric range errors (in m), T is the tropospheric range error (in m), N_{L1} and N_{L2} are the integer ambiguities (in cycles), MP_{P1}, MP_{P2}, $MP_{\phi L1}$ and $MP_{\phi L2}$ are the corresponding pseudorange and carrier phase multipath, respectively (including the observational noise), $\lambda_{L1} \approx 19$ cm and $\lambda_{L2} \approx 24$ cm are the wavelengths of the signals on L1 and L2, $f_1 \approx 1.5754\ GHz$ and $f_2 \approx 1.2276\ GHz$ are frequencies of signals L1 and L2, respectively.

Taking the advantage of the relationship that between the ionospheric delay for L1 and L2 leads to:

$$I_{L2} = \alpha \cdot I_{L1} \tag{5}$$

with:

$$\alpha = \left(\frac{f_1}{f_2} \right)^2 .$$

Subtracting Equation (4) from (3) gives:

$$\Phi_{L1} - \Phi_{L2} = \lambda_{L1} N_{L1} - I_{L1} + MP_{\Phi_{L1}} - \lambda_{L2} N_{L2} + I_{L2} - MP_{\Phi_{L2}} \tag{6}$$

Substituting Equation (5) into (6), grouping and simplifying yields:

$$\frac{(\Phi_{L1} - \Phi_{L2})}{(\alpha - 1)} = I_{L1} + \frac{(\lambda_{L1} N_{L1} - \lambda_{L2} N_{L2})}{(\alpha - 1)} + \frac{(MP_{\Phi_{L1}} - MP_{\Phi_{L2}})}{(\alpha - 1)} \tag{7}$$

Combining Equation (7) with (3) to eliminate I_{L1} term, results in:

$$\begin{aligned} \Phi_{L1} + \frac{(\Phi_{L1} - \Phi_{L2})}{(\alpha - 1)} &= R + c(\quad t^S - \quad t_R) + T + \lambda_{L1} N_{L1} + \\ &\frac{(\lambda_{L1} N_{L1} - \lambda_{L2} N_{L2})}{(\alpha - 1)} + MP_{\Phi_{L1}} + \frac{(MP_{\Phi_{L1}} - MP_{\Phi_{L2}})}{(\alpha - 1)} \\ &= R + c(\quad t^S - \quad t_R) + T + b_1 + m_{\Phi_1} \end{aligned} \tag{8}$$

Equation (8) is a linear combination of observed L1 and L2 carrier phases, where the ambiguity bias term b_1 is introduced as:

$$b_1 = \lambda_{L1} N_{L1} + \frac{(\lambda_{L1} N_{L1} - \lambda_{L2} N_{L2})}{(\alpha - 1)} \tag{9}$$

While the phase multipath effect is now defined by:

$$m_{\Phi_1} = MP_{\Phi_{L1}} + \frac{(MP_{\Phi_{L1}} - MP_{\Phi_{L2}})}{(\alpha - 1)} \quad (10)$$

Combining Equations (3), (7) and (8) gives:

$$P_{L1} - \left[1 + \frac{2}{(\alpha-1)}\right]\Phi_{L1} + \left[\frac{2}{(\alpha-1)}\right]\Phi_{L2} = MP_{P1} - \frac{(\lambda_{L1}N_{L1} - \lambda_{L2}N_{L2})}{(\alpha-1)} - b_1 + MP_{\Phi_{L1}} - 2m_{\Phi_1} \quad (11)$$

The new ambiguity bias term is now defined by:

$$B_1 = -\frac{(\lambda_{L1}N_{L1} - \lambda_{L2}N_{L2})}{(\alpha-1)} - b_1 = -\left[1 + \frac{2}{(\alpha-1)}\right]\lambda_{L1}N_{L1} + \left[\frac{2}{(\alpha-1)}\right]\lambda_{L2}N_{L2} \quad (12)$$

And the new phase multipath effect is introduced as:

$$M_{\Phi 1} = -(MP_{\Phi_{L1}} - MP_{\Phi_{L2}}) - m_{\Phi_1} = -\left[1 + \frac{2}{(\alpha-1)}\right]MP_{\Phi_{L1}} + \left[\frac{2}{(\alpha-1)}\right]MP_{\Phi_{L2}} = MP_{\Phi_{L1}} - 2m_{\Phi_1} \quad (13)$$

The pseudorange multipath MP_1 is then expressed as the linear combination from (11), namely:

$$MP_1 = P_{L1} - \left[1 + \frac{2}{(\alpha-1)}\right]\Phi_{L1} + \left[\frac{2}{(\alpha-1)}\right]\Phi_{L2} = MP_{P1} + B_1 + M_{\Phi_1} \quad (14)$$

Similar derivations are performed to express MP_2 as a linear combination:

$$MP_2 = P_{L2} - \left[\frac{2\cdot\alpha}{(\alpha-1)}\right]\Phi_{L1} + \left[\frac{2\cdot\alpha}{(\alpha-1)} - 1\right]\Phi_{L2} = MP_{P2} + B_2 + M_{\Phi 2} \quad (15)$$

with: MP_{P2}, B_2, and $M_{\phi 2}$ are defined similarly to MP_{P1}, B_1, and $M_{\phi 1}$.

Based on the above derivations, the daily MP1-RMS and MP2-RMS variations were computed by means of Equations (14) and (15).

Results and analysis

Even though TAMDEF network consists of 33-stations, only the "tested" sites with longer GPS data span (FLM2, FTP1, LWN0, MCM4, ROB1 and WHN0) were considered for the analysis, and they are illustrated in Figures 3 and 4. There the daily MP1-RMS (with scatter from 0 to 1 meter) and MP2-RMS (with scatter from 0 to 3 meters) variations are presented in terms of

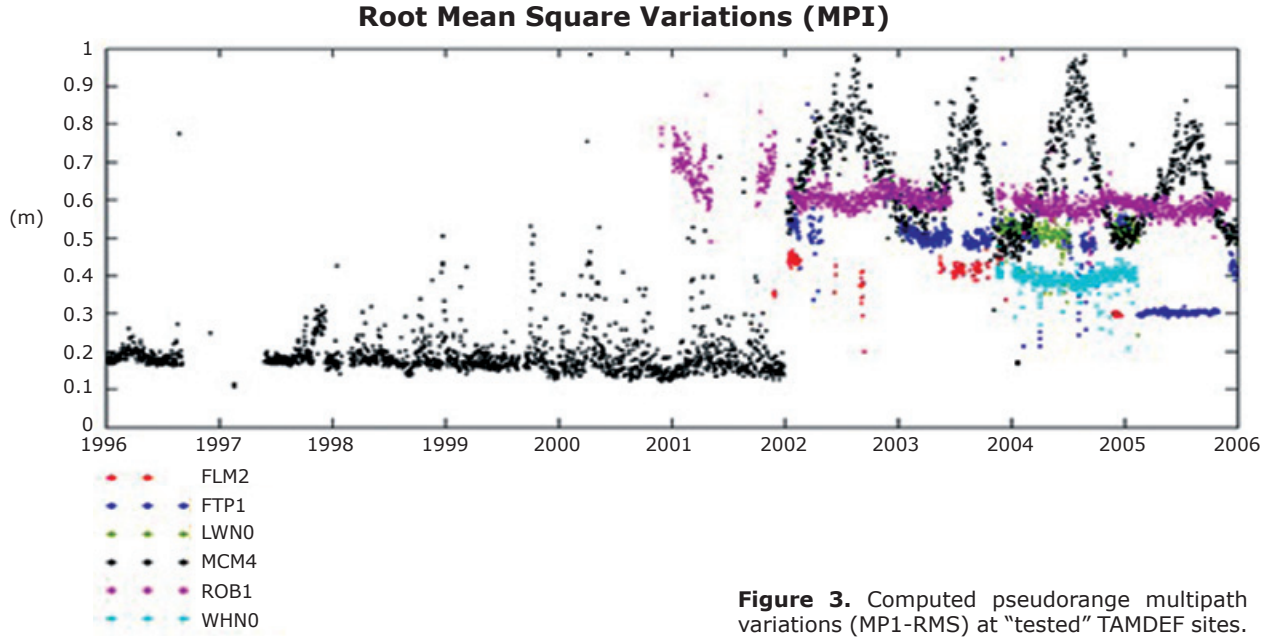

Figure 3. Computed pseudorange multipath variations (MP1-RMS) at "tested" TAMDEF sites.

time-series (1996-2006). As can be seen in these figures, MCM4 is the site with almost 10-years of continuous data. In other words, roughly 3300 days of GPS data were available for this site. However, there is a gap from September 1996 to May 1997; after that date, the MCM4 station recorded data almost for the entire next years. A jump on the MP1-RMS and MP2-RMS results can be observed at the MCM4 site at the beginning of year 2002. This fact could be attributed to the hardware change when the AOA SNR-12 ACT replaced the ROGUE SNR-8000 GPS receiver on January 3, 2002.

It is very important to point out, that there was no antenna replacement since the installation of the MCM4 site and this is illustrated in Figure 5. Also note that seasonal moisture condensation can be seen inside the radome. Furthermore, for the period between 2002 and 2006 (after the receiver replacement issue), the MP1-RMS and MP2-RMS results for MCM4 behave the same way (i.e., annual variations) getting the highest values in the middle of every year. Prior to 2002, the results look much more comparable among them at MCM4.

The MP1-RMS and the MP2-RMS represent the pseudorange multipath variability, for instance, often track the annual variations of heights. Thus, according to Ray (2006) annual heights and MP1-RMS and MP2-RMS variations are sometimes found to be correlated with changes in station tracking hardware, and this is illustrated in Figure 6. Annual signals begin with GPS receiver swap (3 Jan 2002), Turbo Rogue SNR-8000 changed to AOA SNR-12. Scale and units (millimeter) for the height (dU) are shown in the left hand side, while the scale and units (meter level) for the MP1-RMS and MP2-RMS are presented on the right hand side of the figure.

Results for the FLM2, LWN0 and WHN0 sites fluctuate within 20 to 65 centimeters for MP1-RMS and within 0.3 to 1.3 meters for MP2-RMS, respectively; with no significant variations

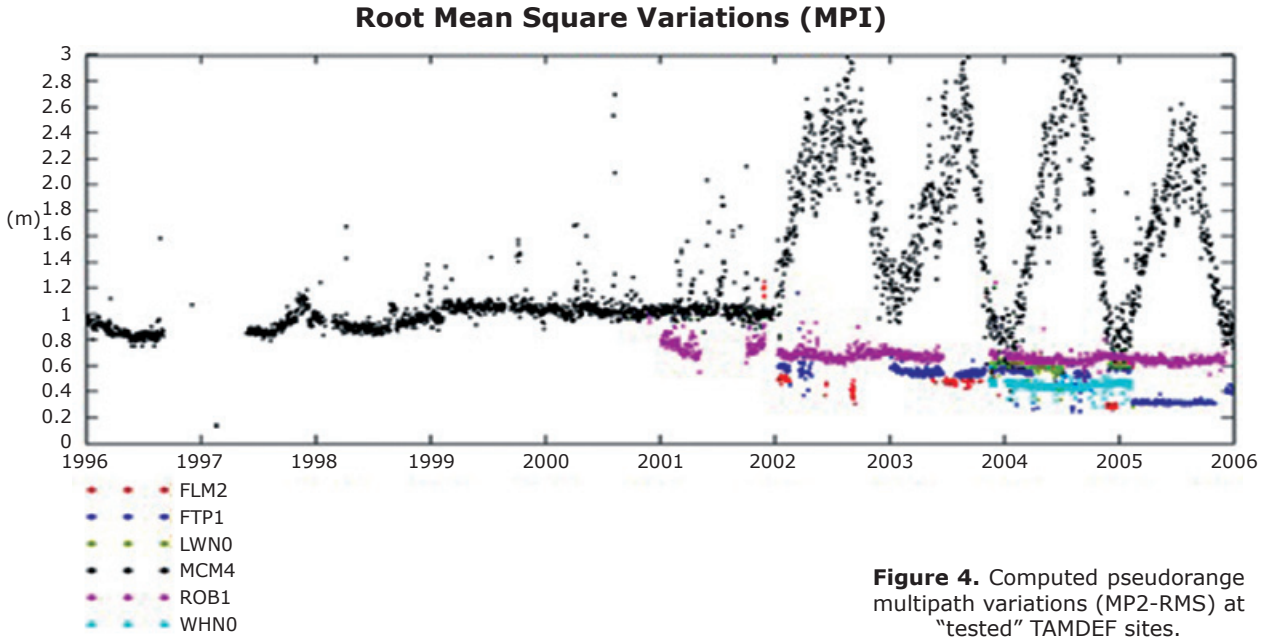

Figure 4. Computed pseudorange multipath variations (MP2-RMS) at "tested" TAMDEF sites.

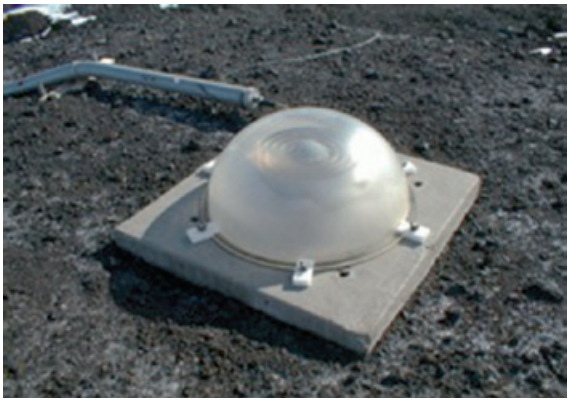

Figure 5. McMurdo (MCM4) IGS and TAMDEF site, primary ITRF access point for this part of Antarctica.

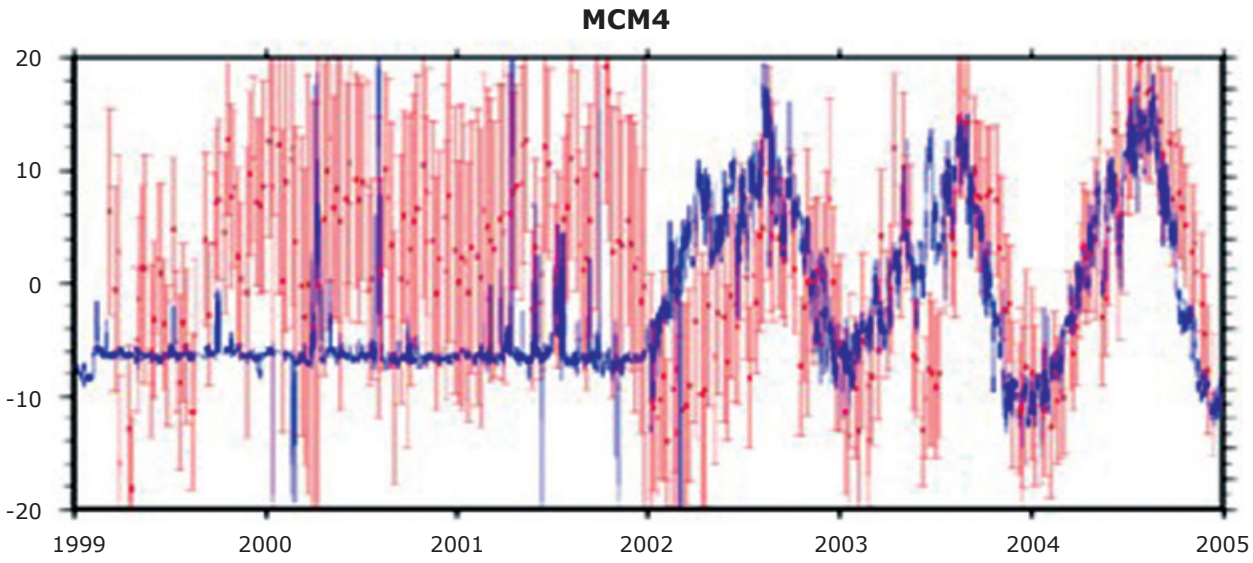

Figure 6. Annual heights vs. MP1-RMS and MP2-RMS at MCM4 site.

in their behavior. However, it is difficult to comment on how these stations performed, since not enough data is available for a better interpretation; except for the WHN0 that shows almost a complete year (316 days) of consistent results for the analysis. Results for the FTP1 site oscillate from 20 to 90 centimeters for MP1-RMS and from 0.25 to 1.15 meters for MP2-RMS, respectively. In addition, FTP1 station presents a discontinuity in the results that can be observed after year 2005. This fact definitely cannot be attributed to any change in the hardware, since no replacement in the antenna or receiver had occurred since the installation of the site. On the other hand, the MP1-RMS variations for ROB1 site ranges from 0.4 to 1 meter, while the scatter for the MP2-RMS is within 0.4 to 1.25 meters and both graphs seem to follow a pattern that also could be considered as sinusoidal, but in a short scale as compared to the MCM4 station. A gap can be observed as well for the ROB1 station for mid 2003 to beginning of year 2004.

Photographs obtained for some of the tested GPS sites (FLM2, FTP1 and ROB1) verified the presence of rocks, solar panels and other reflectors in close proximity to the GPS antennas that could be a potential source of the multipath effect (see Figures 7, 8 and 9). In addition, with knowledge from these photographs and from analyzing pseudorange multipath for TAMDEF network it can be determined which sites were severely affected; thus, with other *in-situ* carrier phase calibration techniques one can experiment to infer how well they perform at these selected tested TAMDEF sites.

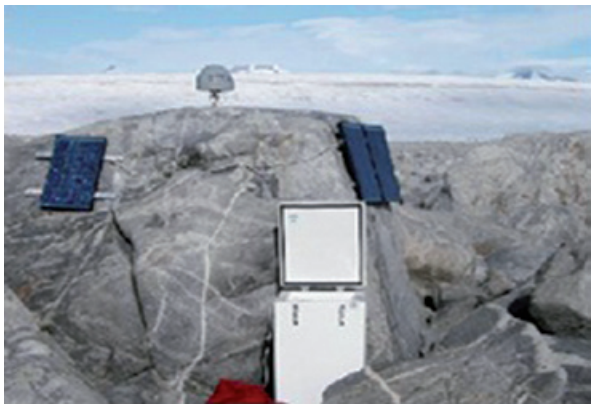

Figure 7. Mount Fleming (FLM2) site, located at the East Antarctic Ice Sheet.

Figure 8. Fishtail Point 1 (FTP1) site, located at the adjacent Ross Sea.

Figure 9. Cape Roberts (ROB1) site, located at the Ross Ice Shelf.

Table 1 and 2 shows the statistics of the MP1-RMS and MP2-RMS variations for all the TAMDEF sites. Here, the maximum, minimum, mean and standard deviations values are presented in units of meters.

In Tables 1 and 2 are sumarized the IGS designator for the hardware used (i.e., GPS receiver and antenna type) as well as the number of available days of data for each TAMDEF. FTP1, MCM4 and ROB1 were the sites with higher levels (meter range) of pseudorange multipath (MP1-RMS), ranking first, second and third as shown in Table 1. Hypothetically, these three stations are within the most affected tested sites with longer data span, even though they rank twenty

Table 1. Statistics of the MP1-RMS for the entire TAMDEF network.

Rank (Order)	Site	No. of Days	Max (m)	Min (m)	St. Dev. ±(m)	Mean (m)	Receiver Type	Antenna Type
1	MCM4	3293	1.76	0.11	0.25	0.40	AOA SNR-12 ACT	AOAD/M_T
2	ROB1	1406	0.97	0.43	0.04	0.60	TPS HE_GD	ASH700936E
3	FTP1	882	0.89	0.21	0.10	0.45	TPS HE_GD	ASH700936D_M
4	WTE0	69	0.85	0.01	0.21	0.54	ASHTECH Z-XII3	TRM29659.00
5	FIE0	266	0.83	0.24	0.05	0.43	TPS HE_GGD	ASH701945B_M
6	KER0	81	0.75	0.22	0.09	0.36	DL4-NovAtel	ASH700936E
7	BRM0	30	0.73	0.23	0.09	0.45	TRIMBLE_5700	ASH701945E_M
8	LWN0	317	0.64	0.24	0.04	0.51	TPS HE_GGD	ASH701945B_M
9	ROY0	69	0.59	0.08	0.12	0.22	TRIMBLE 4000SSI	TRM29659.00
10	BRO0	80	0.57	0.24	0.05	0.33	DL4-NovAtel	ASH700936E
11	WAL0	74	0.55	0.02	0.14	0.20	TRIMBLE 4000SSE	TRM 29659.00
12	BRA0	42	0.52	0.33	0.06	0.47	TRIMBLE 4000SSI	ASH700936E
13	ROS0	33	0.51	0.26	0.05	0.34	DL4-NovAtel	ASH701945D_M
14	MAS0	30	0.51	0.37	0.04	0.42	TRIMBLE 4000SSE	TRM29659.00
15	BIR0	31	0.51	0.08	0.16	0.29	TRIMBLE 4000SSI	ASH700936E
16	CRZ0	19	0.50	0.19	0.09	0.43	TRIMBLE 5700	ASH701945C_M
17	CON0	49	0.49	0.22	0.05	0.28	DL4-NovAtel	ASH700936E
18	WHN0	372	0.48	0.21	0.03	0.39	TPS HE_GGD	ASH701945B_M
19	ALN0	58	0.47	0.19	0.07	0.31	ASHTECH Z-12	ASH700936E
20	FLM2	166	0.47	0.20	0.06	0.39	TPS HE_GD	ASH700936E
21	BUR0	60	0.46	0.24	0.04	0.31	DL4-NovAtel	ASH700936E
22	BFT0	38	0.45	0.23	0.09	0.36	TPS LEGACY	ASH701945E_M
23	WRN0	124	0.43	0.17	0.05	0.27	DL4-NovAtel	ASH700936E
24	ANT0	46	0.40	0.20	0.05	0.29	TRIMBLE 4000SSE	ASH700936E
25	MBF0	74	0.38	0.18	0.06	0.27	TRIMBLE 5700	ASH701945E_M
26	BTL0	29	0.38	0.17	0.05	0.30	ASHTECH Z-12	TRM41249.00
27	ESH0	40	0.37	0.17	0.04	0.24	DL4-NovAtel	NOV702_2.02
28	RYN0	44	0.36	0.27	0.02	0.32	TRIMBLE 5700	ASH701945E_M
29	DWT0	21	0.36	0.21	0.04	0.29	ASHTECH Z-12	ASH700936E
30	VAN0	10	0.35	0.32	0.01	0.33	TRIMBLE 4000SSI	TRM22020.00+GP
31	FRK0	29	0.35	0.20	0.06	0.39	ASHTECH Z-12	ASH700936E
32	FLM0	18	0.31	0.27	0.01	0.29	TPS HE_GD	ASH700936E
33	CRN0	16	0.30	0.27	0.01	0.29	TRIMBLE 4000SSE	ASH700936E

Table 2. Statistics of the MP2-RMS for the entire TAMDEF network.

Rank (Order)	Site	No. of Days	Max (m)	Min (m)	St. Dev. ±(m)	Mean (m)	Receiver Type	Antenna Type
1	MCM4	3293	3.38	0.13	0.56	1.33	AOA SNR-12 ACT	AOAD/M_T
2	ROS0	33	1.59	0.37	0.41	1.10	DL4-NovAtel	ASH701945D_M
3	BTL0	29	1.54	0.26	0.45	0.78	ASHTECH Z-12	TRM41249.00
4	WAL0	74	1.53	0.04	0.36	0.36	TRIMBLE 4000SSE	TRM 29659.00
5	RYN0	44	1.53	0.88	0.15	1.31	TRIMBLE 5700	ASH701945E_M
6	BIR0	31	1.52	0.12	0.51	0.66	TRIMBLE 4000SSI	ASH700936E
7	ESH0	40	1.50	0.24	0.46	0.75	DL4-NovAtel	NOV702_2.02
8	WTE0	69	1.46	0.01	0.30	0.86	ASHTECH Z-XII3	TRM29659.00
9	CRZ0	19	1.46	0.38	0.29	1.12	TRIMBLE 5700	ASH701945C_M
10	MBF0	74	1.45	0.27	0.43	0.70	TRIMBLE 5700	ASH701945E_M
11	BRA0	42	1.45	0.43	0.32	0.76	TRIMBLE 4000SSI	ASH700936E
12	ANT0	46	1.45	0.40	0.28	0.97	TRIMBLE 4000SSE	ASH700936E
13	DWT0	21	1.44	0.44	0.34	1.05	ASHTECH Z-12	ASH700936E
14	MAS0	30	1.43	0.84	0.24	1.17	TRIMBLE 4000SSE	TRM29659.00
15	FRK0	29	1.41	0.33	0.39	0.82	ASHTECH Z-12	ASH700936E
16	CRN0	16	1.40	1.15	0.07	1.30	TRIMBLE 4000SSE	ASH700936E
17	ALN0	58	1.39	0.30	0.40	0.69	ASHTECH Z-12	ASH700936E
18	WRN0	124	1.39	0.35	0.33	0.70	DL4-NovAtel	ASH700936E
19	BRM0	30	1.38	0.51	0.24	1.16	TRIMBLE_5700	ASH701945E_M
20	FLM0	18	1.36	0.38	0.24	1.07	TPS HE_GD	ASH700936E
21	FIE0	266	1.32	0.25	0.08	0.52	TPS HE_GGD	ASH701945B_M
22	FLM2	166	1.25	0.27	0.16	0.47	TPS HE_GD	ASH700936E
23	ROB1	1406	1.24	0.41	0.06	0.68	TPS HE_GD	ASH700936E
24	BFT0	38	1.21	0.49	0.25	0.71	TPS LEGACY	ASH701945E_M
25	FTP1	882	1.16	0.25	0.12	0.48	TPS HE_GD	ASH700936D_M
26	ROY0	69	1.14	0.15	0.24	0.35	TRIMBLE 4000SSI	TRM29659.00
27	KER0	81	0.98	0.54	0.10	0.71	DL4-NovAtel	ASH700936E
28	LWN0	317	0.71	0.28	0.05	0.60	TPS HE_GGD	ASH701945B_M
29	BUR0	60	0.69	0.55	0.03	0.61	DL4-NovAtel	ASH700936E
30	BRO0	80	0.69	0.33	0.06	0.45	DL4-NovAtel	ASH700936E
31	WHN0	372	0.60	0.28	0.03	0.45	TPS HE_GGD	ASH701945B_M
32	VAN0	10	0.58	0.44	0.04	0.53	TRIMBLE 4000SSI	TRM22020.00+GP
33	CON0	49	0.56	0.30	0.05	0.38	DL4-NovAtel	ASH700936E

first, one and twenty third, respectively for MP2-RMS (see Table 2). It is very important to point out here that, following the recommendation provided by Hilla and Cline (2002) the GPS data used to compute the pseudorange multipath results, which are presented in Tables 1 and 2 were not smoothed. In other words, it was ensure that the TEQC software used to generate the MP1-RMS and MP2-RMS variations had turned off the smoothing option; otherwise results tend to look overly optimistic.

Conclusions

Definitely, TAMDEF stations were mostly affected in MP2. This issue could be attributed to the presence of rocks, solar panels and other reflectors nearby to the GPS antennas that could be a potential source of the multipath effect. Other potential issues might be how the GPS antennas were mounted, the antenna type used and its surrounding environment. However, the antenna calibration issue could be another source for having high levels of multipath. Thus, overall it can be concluded that MCM4 was found to be the site with highest multipath (between 1 to 3 meters) for the MP1-RMS and MP2-RMS variations, respectively. This fact is not good at all, since MCM4 is the primary ITRF access point for this part of Antarctica. The reason for high multipath (with seasonal effect) at MCM4 might be due to the receiver itself, the location environment and the existence of the antenna radome. Also recall that MCM4 antenna never has

been calibrated since this was initially installed in 1995. Higher levels of pseudorange multipath were also found for FTP1 and ROB1 sites, which seem not to have a problem with the GPS hardware but perhaps for the antenna environment (rocks and solar panels). Additionally, results from the pseudorange multipath (MP1-RMS and MP2-RMS variations) should be considered for further research to improve positioning results and GPS data cleaning for TAMDEF network.

Bibliography

Dodson A.H., Meng X., Roberts G.W., 2001, Adaptive Method for Multipath Mitigation and Its Applications for Structural Deflection Monitoring. *Proceedings of International Symposium on Kinematic Systems in Geodesy, Geomatics and Navigation*, Banff Alberta, Canada 101-110.

Estey L.H., Meertens C.M., 1999, TEQC: the multi-purpose toolkit for GPS/GLONASS data. GPS Solutions (3)1:42–49.

Ge L., Han S., Rizos C., 2000, Multipath Mitigation of Continuous GPS Measurements Using an Adaptive Filter. *GPS Solutions*, 4(2), 19-30.

Ge L., Han S., Rizos C., 2002, GPS Multipath Change Detection in Permanent GPS Stations. *Survey Review*, 36(283), 306-322.

Han S., Rizos C., 1997, Multipath Effects on GPS in mine environments. *X International Congress of the International Society for Mine Surveying, Fremantle, Australia,* 447-457.

Hilla S., Cline M., 2002, Evaluating Pseudorange Multipath Effects at Stations in the National CORS Network. *Proceedings of the Weiko A. Heiskanen Symposium in Geodesy*, Department of Geodetic Science and Surveying The Ohio State University, Columbus, Ohio, on CD.

Meertens C., 2000, The Antenna and Multipath Calibration System website: http://www.unavco.ucar.edu/projects/active_projects/amcs.

Ray Jim, 2006, Systematic errors in GPS position estimates, *IGS Workshop 2006*, 8-11 May 2006.

Rizos C., 1999, Quality Issues in Real-time GPS Positioning. IUGG Congress, Birmingham, U.K.

Roberts G.W., Meng X., Dodson A.H., Cosser E., 2002, Multipath Mitigation for Bridge Deformation Monitoring. *Journal of Global Positioning System* 1(1), 25-33.

Satirapod C., Khoonphool R., Rizos C., 2003, Multipath Mitigation of Permanent GPS Stations Using Wavelets. *Proceedings of 2003 International Symposium on GPS/GNSS*, Tokyo, Japan, 133-139.

http://www.geology.ohio-state.edu/TerryWilson/research_gps.htm

http://www.polenet.org/

http://www.grdl.noaa.gov/ANTCAL/

ftp://igscb.jpl.nasa.gov/igscb/data/format/rinex210.txt

http://www.unavco.org/facility/software/teqc/teqc.html

http://www.unavco.org QC v3 User Guide, UNAVCO, Document Date: March 1994.